Photochemical Reaction Dynamics Measured using the Near-Field Heterodyne Transient Grating Method

M. Okuda and K. Katayama*

Department of Applied Chemistry, Faculty of Science and Technology, Chuo University, 1-13-27 Kasuga, Bunkyo, Tokyo 112-8551, Japan

Received: December 4, 2007; Revised Manuscript Received: February 22, 2008

The recently developed near-field heterodyne transient grating method was utilized in the analysis of photochemical reaction dynamics. It was applied to the dynamics measurement of the dimerization reaction of anthracene in the temporal range from nanoseconds to milliseconds. By means of wide dynamic range measurements, the relaxation processes of excited states such as the excimer and triplet, and the diffusion process of the photodimer product, could be directly observed. Relative photodimerization efficiency obtained experimentally was compared with the simulation results of the reaction kinetics on the basis of two different reaction schemes—reaction by way of the singlet or triplet excited states—and it was confirmed that this reaction occurs through the singlet excited state.

1. Introduction

The dynamics of a photochemical reaction, such as the formation and extinction of singlet, triplet, or intermediate states, is conventionally observed via transient absorption and time-resolved fluorescence methods. On the other hand, the transient grating (TG) method is also a powerful tool for investigating photochemical reaction dynamics, and it differs from other methods in that the dynamics are detected through the change in the complex refractive index due to photoinduced physical or chemical changes.[1–4] In the TG technique are observed not only the population dynamics of the excited state but also the acoustic and thermal responses that originate because of heat generation, and the obtained information provides a variety of properties such as the lifetime of excited states, the reaction enthalpy, the molar volume, and the diffusion coefficients of reactants, products, and intermediates.[2,5] However, it is sometimes difficult to determine the properties of each dynamic process in the overall transient response, because it includes various processes that originate from the real and imaginary part of the refractive index change. Therefore, the heterodyne detection of a TG signal was employed,[6–10] and the real and imaginary parts of the complex refractive index change ($\Delta n(t)$ and $\Delta k(t)$) were selectively detected by controlling the optical phase of the signal and reference light fields.[11–14] In recent years, two-dimensional IR spectroscopy[15–18] and two-dimensional electronic spectroscopy,[19,20] which are based on three-pulse photon echo spectroscopy or four-wave mixing spectroscopy, have progressed remarkably. In this research field, the type of phase control employed is same as that of the heterodyne detection.

In the conventional TG optical setup, the temporal and spatial control of three short optical pulses is necessary, which is not an easy task for general users. We have recently developed the near-field heterodyne transient grating (NF-HD-TG) method, which features a simple optical setup and highly sensitive detection using a heterodyne technique.[21,22] In a previous paper,[23] it was reported that this method offers a simple separation of the real and imaginary parts of the refractive index change in the range from nanoseconds to milliseconds.

* To who correspondence should be addressed. E-mail: kkatayama@chem.chuo-u.ac.jp.

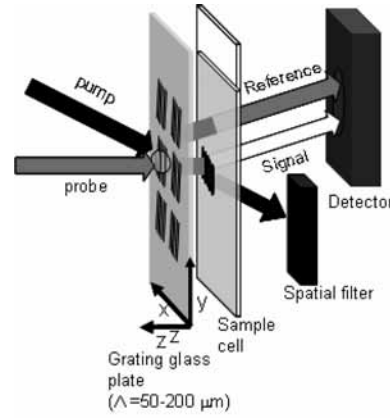

Figure 1. Schematic representation of the optical setup of the NF-HD-TG method. The pump light was tilted downward at an angle of 2.86° to overlap with the probe light at the sample cell. The cell had an internal thickness of 1.5 mm. A transmission grating with various grating spacings (50−200 μm) was used.

In this paper, a practical example of this method for understanding a photochemical reaction was presented. The dimerization reaction of anthracene under ultraviolet irradiation was chosen as a demonstration experiment. The photochemical reaction dynamics of anthracene were observed, and the interconnection between the dynamics in each temporal range was clarified. This reaction is one of the well-known photochemical reactions; it is known to proceed mainly by way of the singlet excited state, and the triplet excited state also sometimes works as a reaction intermediate.[24,25]

2. Principles

Detailed principles of the NF-HD-TG are explained in the aforementioned paper,[23] and a brief explanation is provided here. A schematic diagram of the setup is shown in Figure 1. When a pump beam is incident on a transmission grating, an optical fringe pattern is formed on the opposite side of the diffraction grating. When a liquid sample is placed near the transmission grating, it can be excited by the fringe pattern of the pump light.

10.1021/jp711424b CCC: $40.75
Published on Web 04/24/2008

The refractive index of the liquid changes because of photochemical and photothermal processes that have the same pattern as the optical fringe, and this is called a transient grating. When another light beam (probe light) is incident on the transient grating, it is diffracted both by the transmission grating (reference) and the transient grating (signal). The two diffracted beams are directed in the same direction, and they are detected by a detector positioned at the first-order diffraction spot of the visible reference spot. The detected signal is heterodyned, and its intensity is expressed as

$$I(t) = I_{\mathrm{ref}} + ((\Delta n(t))^2 + (\Delta k(t))^2)I_{\mathrm{pr}} + 2E_{\mathrm{ref}}E_{\mathrm{pr}}(\Delta n(t)\cos(\varphi + \varphi_0) + \Delta k(t)\sin(\varphi + \varphi_0)) \quad (1)$$

where I_{ref} and I_{pr} are the intensities of the reference and probe, respectively, E_{ref} and E_{pr} are the electric fields of the reference and probe, respectively, ϕ is the phase difference between the signal and the reference, Δn and Δk are the real and imaginary parts of the refractive index change, respectively, and ϕ_0 is the initial phase difference. The first term in this expression is a constant background, and the second term (homodyne signal) is usually significantly smaller than the third term (heterodyne signal).[26] The phase difference is varied by varying the optical path difference between the signal and the reference, which can be controlled by changing the distance between the transmission grating and the sample. The phase difference is expressed as

$$\varphi = (2\pi/\lambda_{\mathrm{probe}})\Delta l = d(1/\cos\theta - 1)(2\pi/\lambda_{\mathrm{probe}}) \quad (2)$$

where Δl is the optical path difference between the signal and the reference, d is the grating−sample distance, and θ is a diffraction angle. From eqs 1 and 2, $\Delta n(t)$ or $\Delta k(t)$ can be selectively detected by setting d to appropriate positions.

In the TG responses, various sources for the refractive index change contribute to the signal, and the temporal change of the complex refractive index is expressed as

$$\Delta\tilde{n}(t) = \Delta\tilde{n}_{\mathrm{pop}}(t) + \Delta\tilde{n}_{\mathrm{acoustic}}(t) + \Delta\tilde{n}_{\mathrm{thermal}}(t) \quad (3)$$

where $\Delta\tilde{n}_{\mathrm{pop}}(t)$ is caused by the population change of excited states and $\Delta\tilde{n}_{\mathrm{acoustic}}(t)$ represents the acoustic grating, which is an acoustic wave generated by thermal expansion, whose wavelength is equal to the optical fringe of the pump light. $\Delta\tilde{n}_{\mathrm{thermal}}(t)$ is the thermal grating, which is a temperature rise profile with a stripe pattern whose spacing is equal to the optical fringe of the pump and which decays because of thermal diffusion. In essence, the refractive index change has a real and an imaginary part; however, it is well-known that only the real part is changed by the acoustic grating and thermal grating. The decay of each component is expressed as[27]

$$\Delta n_{\mathrm{acoustic}}(t) = A_1\cos(2\pi ft + \varphi)\exp\left(-\frac{t}{\tau_{\mathrm{ac}}}\right) \quad (4)$$

$$\Delta n_{\mathrm{thermal}}(t) = A_2\exp\left(-D_{\mathrm{th}}\left(\frac{2\pi}{\Lambda}\right)^2 t\right) \quad (5)$$

where A_1 and A_2 are coefficients, f is the oscillation frequency equal to v_{ac}/Λ (Λ = grating spacing; v_{ac} = acoustic velocity of solvent), τ_{ac} is the decay time of the acoustic grating, and D_{th} is the thermal diffusion coefficient of the solvent. The population term in eq 3 can be separated as follows:

$$\Delta\tilde{n}_{\mathrm{pop}}(t) = \Delta\tilde{n}_{S_1}(t) + \Delta\tilde{n}_{T_1}(t) + \Delta\tilde{n}_{\mathrm{int}}(t) + (\Delta\tilde{n}_{\mathrm{rea}}(t) - \Delta\tilde{n}_{\mathrm{pro}}(t)) \quad (6)$$

where the respective components correspond to the population change of the singlet, triplet, intermediate, reactant, and product. In the TG response, the population term decays because of both a relaxation to the ground state and a diffusion in the perpendicular direction of the grating pattern. For the singlet, triplet, and intermediate states, their lifetime is much shorter than the diffusion process, and the corresponding refractive index changes are expressed as

$$\Delta n_{S_1}(t) \text{ or } \Delta k_{S_1}(t) = A_3\exp\left(-\frac{t}{\tau_{S_1}}\right) \quad (7)$$

$$\Delta n_{T_1}(t) \text{ or } \Delta k_{T_1}(t) = A_4\exp\left(-\frac{t}{\tau_{T_1}}\right) \quad (8)$$

$$\Delta n_{\mathrm{int}}(t) \text{ or } \Delta k_{\mathrm{int}}(t) = A_5\exp\left(-\frac{t}{\tau_{\mathrm{int}}}\right) \quad (9)$$

where τ_{S_1}, τ_{T_1}, and τ_{int} are the lifetimes of the singlet, triplet, and intermediate states, respectively. With regard to the population change of the reactant and product terms, the reactants are created and the products are depleted during the course of the photoreaction (species grating). The signal intensity of the species grating is given by the difference between the change in the refractive index due to the reactant ($\Delta\tilde{n}_{\mathrm{rea}}$) and that due to the product ($\Delta\tilde{n}_{\mathrm{pro}}$). The sign of $\Delta\tilde{n}_{\mathrm{pro}}$ is opposite of that for $\Delta\tilde{n}_{\mathrm{rea}}$ because the phase of the spatial concentration modulation is shifted by 180° with respect to that of the reactant. The signal intensity of the species grating becomes weaker as the spatial modulations of the refractive index become uniform, and this is accomplished by translational diffusion in a direction perpendicular to the grating. Since the reactant and product species do not disappear, it is expressed as

$$\Delta\tilde{n}_{\mathrm{rea}}(t) \text{ or } \Delta k_{\mathrm{rea}}(t) = A_6\exp\left(-D_{\mathrm{rea}}\left(\frac{2\pi}{\Lambda}\right)^2 t\right) \quad (10)$$

$$\Delta\tilde{n}_{\mathrm{pro}}(t) \text{ or } \Delta k_{\mathrm{pro}}(t) = A_7\exp\left(-D_{\mathrm{pro}}\left(\frac{2\pi}{\Lambda}\right)^2 t\right) \quad (11)$$

where D_{rea} and D_{pro} are the diffusion coefficients of the reactant and product, respectively, which can be obtained from the dependence of the decay time on the grating spacing.[28]

3. Experiment

The pump light was the third harmonic of a Nd:YAG laser (GAIA, Rayture Systems Inc.) with a wavelength of 355 nm, a repetition rate of 1−20 Hz, a pulse width of 4 ns, and a pulse energy of less than 0.5 mJ/pulse. The probe light was the second harmonic of a CW Nd:YAG laser with a wavelength of 532 nm. The optical setup is shown in Figure 1. The probe light was level with the optical bench and incident onto a sample cell, and the pump light was tilted downward at an angle of 2.86° to overlap with the probe light at the sample cell. The cell had an internal thickness of 1.5 mm. A transmission grating with various grating spacings (50−200 μm) was fabricated on a Pyrex glass plate and placed in front of the sample cell. After the pump and probe beams passed through the sample cell, the pump beam, along with the zeroth-order diffraction of the probe beam, was blocked by a spatial filter to selectively detect the first-order diffraction. One of the probe diffraction beams was detected by a fast photodetector. The detected responses were stored in a digital oscilloscope. Anthracene (Kanto Chemical)/cyclohexane with a concentration of 1−15 mM was used as a sample, and nitrobenzene (Kanto Chemical)/cyclohexane was used as a reference sample. Nitrobenzene is known as a thermal reference, because all the energy absorbed by it is released in the form of heat within 1 ns. In the measurements, the pump pulse irradiation on a spot was applied less than 50 times to

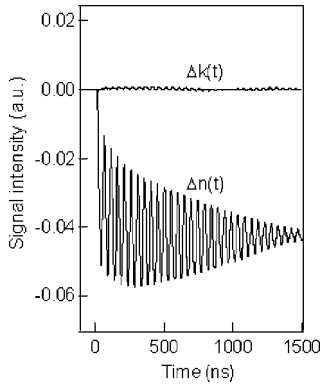

Figure 2. Typical example of the responses of the NF-HD-TG signal for $\Delta n(t)$ and $\Delta k(t)$. The sample used was an anthracene/cyclohexane solution (15 mM).

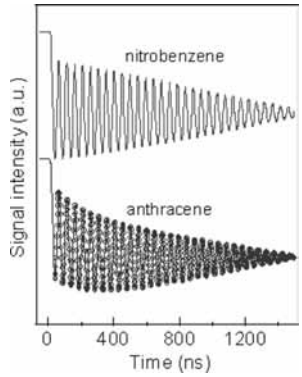

Figure 3. Transient responses for anthracene and nitrobenzene/cyclohexane solutions (15 mM) in the nanosecond order obtained via the NF-HD-TG method. The response for the nitrobenzene solution was fitted with the sum of the components expressed in eqs 4 and 5, and that for the anthracene solution can be fitted with an additional exponential component. The fitting curve for the anthracene solution is also shown.

prevent the accumulation of generated products within the spot area, where the concentration change of the anthracene was less than 5%.

4. Results

Initially, the dimerization reaction was confirmed by analyzing the photochemical products under the laser conditions used with the NF-HD-TG method. The IR spectrum of the anthracene solution (15 mM) showed an absorption band at 1447 cm^{-1} (C−H bending). After the pump pulse laser irradiation was applied to the sample for more than a few minutes, the formation of a crystal was found in the sample cell. The IR spectrum of this crystal showed a split band peak at 1452 and 1473 cm^{-1}, which indicates the presence of a photodimer.[24]

From eq 2, the transient responses of $\Delta n(t)$ and $\Delta k(t)$ are obtained for $\varphi + \varphi_0 = n\pi$ and $\varphi + \varphi_0 = (n + {}^1/_2)\pi$, respectively. Typical examples of the responses for $\Delta n(t)$ and $\Delta k(t)$ are shown in Figure 2. For this sample, the transient signals due to $\Delta k(t)$ were much smaller than those of $\Delta n(t)$ over the entire time range of measurement. Subsequently, the $\Delta n(t)$ responses were shown in the following results.

The transient responses for the anthracene and nitrobenzene solutions in the nanosecond order are shown in Figure 3. Both responses show oscillating decays within the same oscillation period, and the oscillation signals correspond to the acoustic grating, whose frequency agreed with the value predicted from eq 4. It is clear from Figure 3 that there is another response

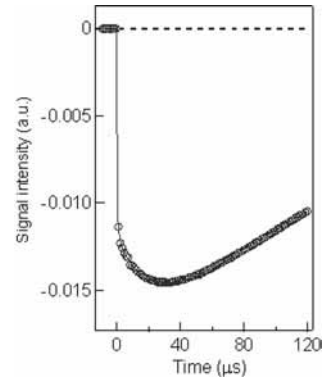

Figure 4. Transient response for the anthracene/cyclohexane solution (15 mM) in the microsecond order obtained via the NF-HD-TG method. The response for the anthracene solution was fitted with the sum of the components, eqs 5 and 8, and the fitting curve is also shown.

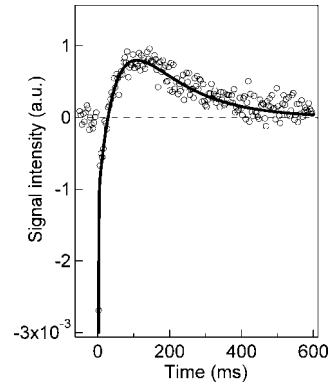

Figure 5. Transient response for the anthracene/cyclohexane solution (15 mM) in the millisecond order obtained via the NF-HD-TG method. The slower part of the response was fitted using eq 11, and the fitting curve is also shown.

within several hundreds of nanoseconds only for the anthracene solution. The response for the nitrobenzene solution can be fitted with the sum of the thermal and acoustic grating components expressed in eqs 4 and 5, while that for the anthracene solution can be fitted with an additional exponential component. Since the signal due to the thermal grating decays for a few milliseconds for the grating spacing used (60 μm), eq 5 is regarded as a constant parameter in the nanosecond order. The decay time for the additional exponential component in the fitting for the anthracene solution was 2.0×10^2 ns. As expected in the theory, this decay time did not depend on the grating spacing.

The transient response for the anthracene solution in the microsecond order is shown in Figure 4. In this time region, the thermal and population gratings of the triplet state contribute to the response. Since it is confirmed from the diffusion coefficient of the solvent (cyclohexane) that the decaying component corresponds to thermal diffusion, the faster component corresponds to the population grating of the triplet. The response was fitted with the sum of the components: eqs 5 and 8. The obtained triplet decay time was 24 μs. This decay time also did not depend on grating spacing.

The transient response for the anthracene solution in the millisecond order is shown in Figure 5. After the signal decay of the thermal diffusion process, the two slower components were observed. Typically, the dynamics that are slower than the decay due to the thermal grating correspond to the chemical species grating (eqs 10 and 11), which decays because of the diffusion of the chemical species. The slower part of the

SCHEME 1: Kinetic Scheme of the Photodimerization of Anthracene by Way of the Singlet Excited State

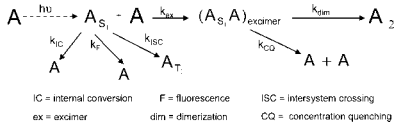

SCHEME 2: Kinetic Scheme of the Photodimerization of Anthracene by Way of the Triplet Excited State

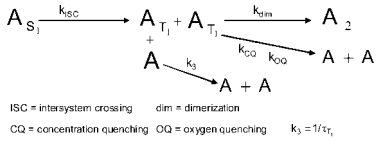

response was fitted with eqs 10 and 11, and the decay time were 50 ms and 1.8×10^2 ms, respectively. These decay times depended on the grating spacing; the diffusion coefficients were obtained from the grating spacing dependence, and they were 1.3×10^{-9} and 3.3×10^{-10} m^2/s, respectively.

5. Discussion

The dimerization reactions of anthracene by ultraviolet irradiation (300−400 nm) have been studied by many researchers, and a reaction mechanism was proposed on the basis of the results of fluorescence quenching at low temperature[29–31] and the quantum yield of photodimers,[32–34] the summary of which is provided in Scheme 1. In this process, an anthracene molecule in the singlet excited state encounters another molecule in the ground state, and these couple to form an excimer. A fraction of the excimers become photodimers, thus competing with the quenching reaction.

It is known that there is another reaction channel by way of the triplet excited state for this reaction.[24,25] The reaction process is summarized in Scheme 2. In this process, two molecules in the triplet excited state encounter one another and change into a photodimer.

Since it is known that the lifetime of the singlet state is 4 ns[24] and that of the triplet state is on the order of microseconds,[35,36] the decay component with a time constant of 2.0×10^2 ns, obtained from Figure 3, corresponds neither to the singlet state nor to the triplet state. Thus, considering Schemes 1 and 2, only the excimer can be a candidate for the decay. Therefore, it is supposed that it corresponds to the excimer decay process due to the dimerization reaction (k_{dim}) and concentration quenching (k_{cq}). With regard to the lifetime of the triplet state obtained from Figure 4, the decay time was shorter with an increase in the anthracene concentration. This result agrees with the fact that the triplet lifetime decreases because of self-quenching for a concentration of more than 5 mM.[24] Furthermore, it was confirmed that the lifetime increased by substituting dissolved oxygen with nitrogen, and this result also supports that this component corresponds to the triplet lifetime, because it is known that the triplet lifetime is subject to the concentration of dissolved oxygen. It can therefore be reasonably concluded that the decays of 50 and 1.8×10^2 ms observed in Figure 5 are due to the diffusion of anthracene and photodimer products, because no other chemical species was generated in this reaction. It is reasonable to suppose that the slower diffusion coefficient corresponds to the dimer of anthracene. The diffusion coefficient for the dimer was about one-fourth of that for anthracene.

The mechanism of the dimerization processes was also analyzed here. The kinetic equations of Schemes 1 and 2 are expressed as follows.

For Scheme 1:

$$\begin{aligned}
&\frac{d[A_{S_1}]}{dt} = -k_1[A_{S_1}] - k_{ex}[A_{S_1}]\,[A] \\
&\frac{d[A]}{dt} = k_1[A_{S_1}] - k_{ex}[A_{S_1}]\,[A] + 2k_{CQ}[A_{S_1}A] \\
&[A_{S_1}]\,[A] \\
&\frac{d[A_{S_1}A]}{dt} = k_{ex}[A_{S_1}]\,[A] - (k_{CQ} + k_{dim})[A_{S_1}A] \\
&\frac{d[A_2]}{dt} = k_{dim}[A_{S_1}A] \\
&k_1 = k_{IC} + k_F + k_{isc}
\end{aligned} \tag{12}$$

For Scheme 2:

$$\begin{aligned}
&\frac{d[A_{T_1}]}{dt} = -k_3[A_{T_1}][A] - k_{dim}[A_{T_1}]^2 \\
&\frac{d[A]}{dt} = k_3[A_{T_1}][A] + 2k_{CQ}[A_{T_1}][A_{T_1}] \\
&\frac{d[A_2]}{dt} = k_{dim}[A_{T_1}][A_{T_1}]
\end{aligned} \tag{13}$$

where $[A]$ is the anthracene concentration, $[A_{S_1}]$, $[A_{S_1}A]$, and $[A_{T_1}]$ are the concentrations of the singlet, excimer, and triplet states, respectively, and $[A_2]$ is the dimer concentration. Using the parameters in the literature,[24] these two cases were simulated under typical initial conditions for these measurements: $[A_{S_1}] = [A_{S_1}]_0 = 1/1000[A]_0$, $[A] = [A]_0 - [A_{S_1}]_0$, and $[A]_0 = 15$ mM for Scheme 1 and $[A_{T_1}] = [A_{T_1}]_0 = 1/1000 \times 0.76$ ($\Phi_{T_1} = 0.76$),[37,38] $[A] = [A]_0 - [A_{T_1}]_0$, and $[A]_0 = 15$ mM for Scheme 2. In the simulation of Scheme 2, the concentration of the singlet excited state was neglected, because this is almost zero in the time region of this scheme. Since there are no experimental data sets of k_3, k_{dim}, and k_{CQ} for Scheme 2, these were adjusted so that the concentration of the triplet excited state decreases with the experimentally obtained decay time. Typical simulation results are shown in parts a and b of Figure 6. From this simulation, we can determine the amount of photodimer products, because the concentration of photodimer products can be obtained after the reaction reaches equilibrium in this simulation for both Schemes 1 and 2.

In the NF-HD-TG experiments, the relative amount of photodimers can be found from the pre-exponential factor, A_7, of the species grating shown in eq 9. The relation for A_6 dependence on the initial concentration of anthracene, $[A]_0$, was obtained, and the experimental variations of $1/[A]_0$ versus the inverse of the A_6 values are shown in Figure 7. The simulated variation of $1/[A]_0$ versus the inverse of the concentration of photodimers is also shown in Figure 7. In these simulations, the inverse of the photodimer concentration showed a linear relationship with $1/[A]_0$ in Scheme 1, while it was almost constant and independent of $1/[A]_0$ in Scheme 2. It is clear that the tendency of the experimental result agrees with the simulation result of Scheme 1. Therefore, it can be safely concluded that this reaction proceeds by way of the singlet excited state. The reaction mechanism of anthracene dimerization processes obtained from our experiments is summarized in Scheme 3.

6. Conclusion

The reaction mechanism of the photodimerization of anthracene was measured using the NF-HD-TG method, and it was confirmed that the main reaction occurs by way of the singlet excited state. Using the NF-HD-TG method, we could observe the reaction dynamics of the excimer, triplet, and photodimer products directly. Furthermore, it is noteworthy that the direct observation of excimers other than under low-temperature conditions has not yet been

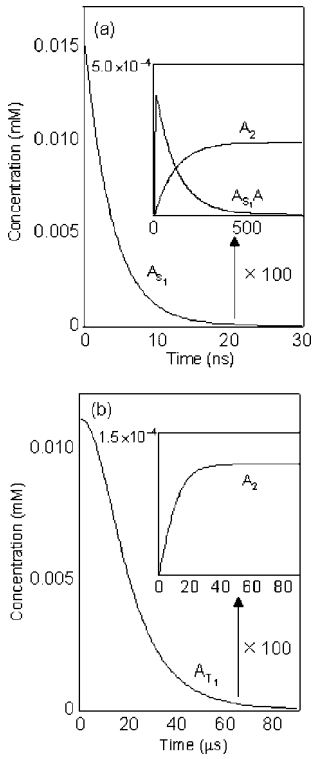

Figure 6. Typical simulation results of the reaction kinetics of anthracene photodimerization: the temporal concentration change of molecules of excited states and photodimers, calculated on the basis of (a) eq 10 and (b) eq 11, respectively. Initial conditions for the simulations were as follows: (a) $[A]_0 = 15$ mM, $[A_{S_1}] = 1.5 \times 10^{-5}$ mM, $k_1 = 2.5 \times 10^8$ s^{-1}, $k_{ex} = 5.0 \times 10^8$ M^{-1} s^{-1}, $k_{CQ} = 4.0 \times 10^6$ M^{-1} s^{-1}, and $k_{dim} = 5.0 \times 10^6$ M^{-1} s^{-1} for Scheme 1; (b) $[A]_0 = 15$ mM, $[A_{T_1}] = 1.1 \times 10^{-5}$ mM, $k_3 = 4.0 \times 10^4$ s^{-1}, $k_{ex} = 3.0 \times 10^4$ M^{-1} s^{-1}, $k_{CQ} = 5.0 \times 10^{14}$ M^{-1} s^{-1}, and $k_{dim} = 8.0 \times 10^4$ M^{-1} s^{-1} for Scheme 2.

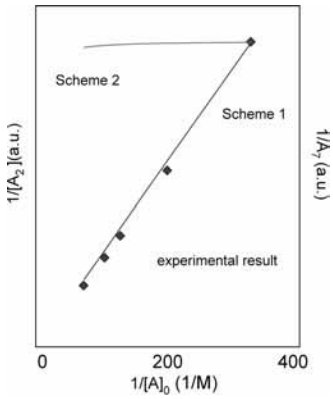

Figure 7. Relation between $1/[A]_0$ versus the inverse of the photodimer concentration for Schemes 1 and 2. The experimental variations of $1/[A]_0$ versus the inverse of the A_7 values are also plotted for comparison.

SCHEME 3: Summary of the Dimerization Reaction of Anthracene Obtained from Our Experiments

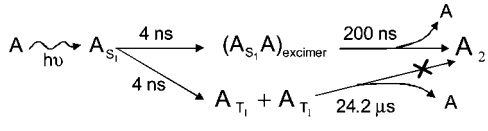

reported, because of their instability and low efficiency of formation. Using this technique, it is possible to understand the overall processes of many photochemical reactions occurring simultaneously using the direct measurements of various intermediate species via wide dynamic range measurements. Another point that should be noted is that every signal in this reaction was found mainly in the real part of the refractive index change, while signals were very small in the imaginary part of the refractive index change. It is supposed that the selection of either the real or the imaginary part of the refractive index change according to the chemical species involved in the reactions is important for detection of photochemical species, and their separation by this technique will help further our understanding of the reaction dynamics.

Acknowledgment. This research was financially supported by a Grant-in-Aid for Scientific Research from the Japan Society for the Promotion of Science.

References and Notes

(1) Nicolet, O.; Vauthey, E. *J. Phys. Chem. A* **2002**, *106*, 5553.
(2) Terazima, M. *J. Photochem. Photobiol. C* **2002**, *3*, 81.
(3) Greenfield, S. R.; Sengupta, A.; Stankus, J. J.; Terazima, M.; Fayer, M. D. *J. Phys. Chem.* **1994**, *98*, 313.
(4) Cho, M. *J. Chem. Phys.* **2001**, *114*, 8040.
(5) Muller, P. A.; Vauthey, E. *J. Phys. Chem. A* **2001**, *105*, 5994.
(6) Goodno, G. D.; Dadusc, G.; Miller, R. J. D. *J. Opt. Soc. Am. B* **1998**, *15*, 1791.
(7) Xu, Q. H.; Ma, Y. Z.; Fleming, G. R. *Chem. Phys. Lett.* **2001**, *338*, 254.
(8) Torre, R.; Taschin, A.; Sampoli, M. *Phys. Rev. E* **2001**, *64*, 061504.
(9) Terazima, M. *Chem. Phys. Lett.* **1999**, *304*, 343.
(10) Vaughan, J. C.; Feurer, T.; Nelson, K. A. *Opt. Lett.* **2004**, *29*, 2052.
(11) Xu, Q. H.; Ma, Y. Z.; Stopkin, I. V.; Fleming, G. R. *J. Chem. Phys.* **2002**, *116*, 9333.
(12) Terazima, M. *J. Phys. Chem. A* **1999**, *103*, 7401.
(13) Goodno, G. D.; Astinov, V.; Miller, R. J. D. *J. Phys. Chem. A* **1999**, *103*, 10630.
(14) Yeremenko, S.; Pshenichnikov, M. S.; Wiersma, D. A. *Phys. Rev. A* **2006**, *73* (2), 021804.
(15) Jonas, D. M. *Annu. Rev. Phys. Chem.* **2003**, *54*, 425.
(16) Khali, M.; Demirdoven, N.; Tokmakoff, A. *J. Phys. Chem. A* **2003**, *107*, 5258.
(17) Zanni, M. T.; Asplund, M. C.; Hochstrasser, R. M. *J. Chem. Phys.* **2001**, *114*, 4579.
(18) Zheng, J.; Kwak, K.; Fayer, M. D. *Acc. Chem. Res.* **2007**, *40*, 75.
(19) Brixner, T.; Stenger, J.; Vaswani, H. M.; Cho, M.; Blankenship, R. E.; Fleming, G. R. *Nature* **2005**, *434*, 625.
(20) Cowan, M. L.; Ogilvie, J. P.; Miller, R. J. D. *Chem. Phys. Lett.* **2004**, *386*, 184.
(21) Katayama, K.; Yamaguchi, M.; Sawada, T. *Appl. Phys. Lett.* **2003**, *82*, 2775.
(22) Yamaguchi, M.; Katayama, K.; Sawada, T. *Chem. Phys. Lett.* **2003**, *377*, 589.
(23) Okuda, M.; Katayama, K. *Chem. Phys. Lett.* **2007**, *443*, 158.
(24) Bouas-Laurent, H.; Castellan, A.; Desvergne, J. P.; Lapouyade, R. *Chem. Soc. Rev.* **2001**, *30*, 248.
(25) Fukuzumi, S.; Okamoto, T.; Ohkubo, K. *J. Phys. Chem. A* **2003**, *107*, 5412.
(26) Terazima, M. *J. Phys. Chem. A* **1999**, *103*, 7401.
(27) Terazima, M. *Chem. Phys.* **1994**, *189*, 793.
(28) Okamoto, K.; Terazima, M.; Hirota, N. *J. Chem. Phys.* **1995**, *103*, 10445.
(29) Bouas-Laurent, H.; Castellan, A.; Desvergne, J.-P. *Pure Appl. Chem.* **1980**, *52*, 2633.
(30) Ferguson, J. *Chem. Rev.* **1986**, *86*, 957.
(31) Bouas-Laurent, H. Desvergne, J.-P. In *Photochromism: Molecules and Systems*; Durr, H., Bouas-Laurent, H., Eds.; Elsevier: Amsterdam, 1990; Chapter *14*, p 561.
(32) Cowan, D. O.; Drisco, R. L. *Elem. Mol. Photochem.* **1976**, *2*, 19.
(33) Castellan, A.; Lapouyade, R.; Bouas-Laurent, H. *Bull. Soc. Chim. Fr.* **1976**, 201.
(34) Becker, H. D. *Advances in Photochemistry*; Volman, D. H., Hammond, G. S., Gollnick, K., Eds.; Wiley: New York, 1990; Vol. 15, p 139.
(35) Nielsen, B. R.; Jorgensen, K.; Skibsted, L. H. *J. Photochem. Photobiol. A* **1998**, *112*, 127.
(36) Jackson, G.; Livingston, R.; Pugh, A. C. *Trans. Faraday Soc.* **1969**, *56*, 1635.
(37) Nijegorodov, N. I.; Downey, W. S. *J. Phys. Chem.* **1994**, *98*, 5639.
(38) Detoma, R. P.; Cowan, D. O. *J. Am. Chem. Soc.* **1975**, *97*, 3283.

JP711424B